ELSEVIER

Chemical Engineering Journal 68 (1997) 87–94

Chemical Engineering Journal

Kinetic study of the direct causticization reaction involving titanates and titanium dioxide

Magnus Palm, Hans Theliander *

Department of Chemical Engineering Design, Chalmers University of Technology, S-412 96 Göteborg, Sweden

Received 1 December 1996; revised 17 March 1997; accepted 26 March 1997

Abstract

The solid state reaction between titanium dioxide and sodium carbonate forming sodium titanates was investigated. Reactions between sodium carbonate and titanium dioxide and/or sodium tri-titanate play a key role in the direct causticization of kraft black liquor. Experiments were carried out in a microdifferential reactor made of quartz glass at varying temperatures up to a maximum of 880 °C. Kinetic data were obtained by measuring the release of carbon dioxide. The physical and chemical properties of the reactants and products were analysed in order to obtain a maximum understanding of the reaction path. Scanning electron microscopy (SEM) and the specific surface area of the reactants and products were applied for morphology determination. X-Ray diffraction (XRD) was employed to characterize the phase composition of the product. The results showed that 100% conversion can be obtained at temperatures above 830 °C. Different kinetic models were taken into consideration, such as the Jander and Valensi–Carter models for diffusion-controlled reaction rates and the phase-boundary model for first-order reaction kinetics. One model was based on the theory that the kinetics can be described by the phase-boundary theory at the beginning of the reaction but, as the reaction proceeds, the rate becomes diffusion controlled. This model gave a good fit to the experimental data collected at 840 °C. However, this model did not work as well at high temperature (880 °C) or at lower temperatures as at 840 °C. This was explained by the fact that the reaction path is different at these temperatures, i.e. other reaction products are involved.

Keywords: Kinetics; Sodium carbonate; Solid state reaction; Titanates; Titanium dioxide

1. Introduction

1.1. Direct causticization

Virtually all the pulp mills in operation in the world today are based on the conventional process of black liquor recovery. The conventional recovery process gives satisfactory chemical recovery, but there are certain drawbacks, e.g. high capital cost, smelt–water explosion hazard and the corrosive nature of the smelt. The industry has been searching for new ways of recovering the chemicals used in the pulping process for more than 25 years. Certain processes, including direct causticization, are considered to be promising alternatives.

A direct alkali recovery system (DARS) was developed and patented in the late 1970s [1,2], whereby the black liquor from the soda process is evaporated and burned with ferric oxide in a furnace/reactor. The product is then fed into a leacher where sodium hydroxide is regenerated. The DARS process is operated commercially at Burnie Mill in Tasmania, Australia [3]. The most important benefits of this process, compared with the conventional one, are that it is safe and easy to operate, harmful emissions are very small and the sodium hydroxide of the white liquor can be controlled to almost any concentration up to 300 g l^{-1} [3].

The DARS process cannot be used for kraft black liquor (KBL) since the ferric oxide reacts with the sulphur-containing compounds in the KBL to form ferric sulphides. Therefore, during the last 20 years, a lot of effort has been placed into finding a compound that can be used in the direct causticization of KBL. The most (and probably the only) suitable direct causticization agents are titanium dioxide (TiO_2) and titanates. Studies of the direct causticization reaction with titanium dioxide have been carried out [4,5].

In a modern concept of KBL recovery, shown in Fig. 1, the conventional causticization step is replaced by direct causticization in the gasifier, where sodium carbonate reacts with added titanium dioxide or recycled sodium tri-titanate to form solid sodium titanate ($4Na_2O \cdot 5TiO_2$). The temperature should be over 840 °C in order to achieve sufficiently high reaction rates [5]. The sodium titanates produced are

* Corresponding author. Fax: 004631814620.

1385-8947/97/$17.00
PII S1385-8947(97)00050-8

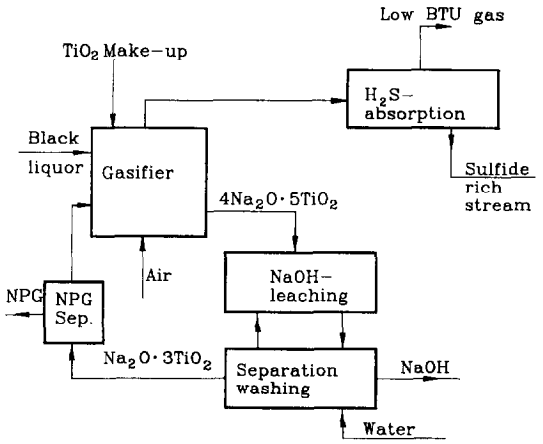

Fig. 1. A KBL gasification process with direct causticization in the fluidized bed.

still solid at these high temperatures, and so smelt formation is prevented. The reactions involved are considered to be

$$Na_2CO_3(s) + 3TiO_2(s) = Na_2O \cdot 3TiO_2(s) + CO_2(g) \quad (1)$$

$$7Na_2CO_3(s) + 5(Na_2O \cdot 3TiO_2)(s) = 3(4Na_2O \cdot 5TiO_2)(s) + 7CO_2(g) \quad (2)$$

The reactions including sulphur are proposed to be

$$Na_2SO_4(s) + 4H_2 = Na_2S(s) + 4H_2O \quad (3)$$

$$Na_2S(s) + CO_2 + H_2O = Na_2CO_3(s) + H_2S \quad (4)$$

The sodium hydroxide is regenerated in the leacher

$$3(4Na_2O \cdot 5TiO_2)(s) + 7H_2O = 14NaOH(aq) + 5(Na_2O \cdot 3TiO_2)(s) \quad (5)$$

The tri-titanate is recycled to the gasifier/reactor. The H_2S is separated from the gasification gas and the aqueous sulphur-rich stream is sent back to the pulping process.

The characteristics and thus economy of this process depend on the causticization reactions, and so it is essential to understand these reactions and to develop reaction models.

1.2. The direct causticization reactions

The reaction between titanium dioxide and sodium carbonate has been studied previously [5]. Using thermogravimetric and differential thermal analysis (TG and DTA) methods, Zou [5] found distinct weight losses at 655, 750 and 985 °C for a mixture of sodium carbonate and titanium dioxide with a molar ratio of unity in air. The weight loss at 985 °C was smaller than the first two. The first weight loss was assumed to be a result of reaction (1).

The second weight loss was considered to be the result of further reaction with the tri-titanate according to reaction (2).

Finally, the reaction of the third weight loss was suggested to be

$$4Na_2O \cdot 5TiO_2 + Na_2CO_3 = 5Na_2O \cdot TiO_2 + CO_2 \quad (6)$$

The validity of these three reactions was confirmed by X-ray diffraction (XRD) analysis, the magnitude of the weight losses and earlier investigations. It is worth noting that most of the sodium carbonate is converted below its melting point (858 °C), indicating that the reaction can be carried out successfully in the solid state. Bamberger and Begun [6] investigated the reaction between Na_2CO_3 and TiO_2 at 700 °C and obtained a product consisting of $Na_2O \cdot 3TiO_2$ and $4Na_2O \cdot 5TiO_2$. This confirms that these are the products at this temperature, as suggested by Zou [5].

Belayev [7] found only meta-titanate ($Na_2O \cdot TiO_2$) as a product when heating equimolar mixtures of sodium carbonate and titanium dioxide above 850 °C. This confirms that reaction (6) is valid. Kiiskilä [4] showed experimentally that, if the reaction atmosphere is changed to CO_2, the equilibrium of reaction (6) is shifted strongly to the left-hand side, in the temperature range 850–950 °C. This was confirmed by Zou [5] who found that meta-titanate is not formed as a product when heating the sample in a CO_2 atmosphere.

This paper presents a study of reactions (1) and (2), where titanium dioxide and sodium carbonate have been used as base materials. The reaction between sodium carbonate and sodium tri-titanate is more important in the industrial process but, according to earlier studies [5], the two reactions show strong similarities.

2. Theory

Most solid state reactions are, to a large extent, controlled by diffusion, i.e. the rate-limiting step is the diffusion of one reactant through the product layer to the other reactant. Studies of systems similar to that involving titanium dioxide and sodium carbonate have shown diffusion-controlled kinetics [7–14]. The studies by Zou [5] indicate that this is also likely to be the case for the reaction between titanium dioxide and sodium carbonate.

Table 1
Three kinetic models based on diffusion as the rate-limiting step

Model	Differential equation	Reference
Jander	$\frac{dr}{dt} = -\frac{k_1}{r_0 - r}$	[12]
Ginstling–Brounstein	$\frac{dr}{dt} = -k_2 \frac{r_0}{r(r_0 - r)}$	[15]
Valensi–Carter	$\frac{dr}{dt} = -k_3 \times \left\{ r - \frac{r^2}{[zr_0^3 + r^3(1-z)]^{1/3}} \right\}^{-1}$	[16]

All models assume spherical particles. r is the radius of the shrinking core of the reactant, r_0 is the initial radius of the particle, z is the ratio of equivalent volumes and t is the time. k_1, k_2 and k_3 are rate constants.

The most common models based on diffusion-controlled kinetics are shown in Table 1, the Jander model being the simplest and the Valensi–Carter model the most advanced. All of these models assume spherical particles and are known as "shrinking core" models, i.e. they assume a shrinking homogeneous core of reactant surrounded by a homogeneous shell of product. All of the models are derived from Fick's second law of diffusion. In the following presentation of these models, the expressions of the rate constants are the same but, as in this case they can only be determined empirically, they differ from one model to another and therefore have different indices. Stoichiometric coefficients may also appear in the expressions for the rate constants but, in the following presentation, this will not be taken into account since the rate constants can only be determined empirically.

2.1. The Jander model

This model is based on diffusion through a plane sheet, where the extension to spherical geometry is made by approximating the spherical shell as a plane sheet. The differential equation in Table 1 is often referred to as the "parabolic law". The Jander model is mostly used in its integrated form

$$[1-(1-x)^{1/3}]^2=\frac{2k_1}{r_0^2}t \tag{7}$$

where x is the degree of conversion. The total radius of the particle (reactant plus product) (r_0) is assumed to be constant. The rate constant is expressed as

$$k_1=\frac{D(c_2-c_1)}{\rho} \tag{8}$$

where D is the diffusivity of the reactant in the product, c_1 is the concentration of the reactant on the inner interface, c_2 is the concentration of the reactant on the outer interface and ρ is the molar density of the reactant in the core.

2.2. The Ginstling–Brounstein model

For radial steady state diffusion in a sphere, Fick's second law is

$$0=D\left(\frac{\partial^2 c}{\partial r}+\frac{2}{r}\frac{\partial c}{\partial r}\right) \tag{9}$$

Eq. (9) is easily solved with the boundary condition that the reactant concentration is constant at all times on the phase boundaries. Combining the solution with a mass balance, the Ginstling–Brounstein model is obtained

$$\frac{dr}{dt}=-k_2\frac{r_0}{r(r_0-r)} \tag{10}$$

where the rate constant is expressed as for the Jander model

$$k_2=\frac{D(c_2-c_1)}{\rho} \tag{11}$$

Just as in the Jander model, the total particle radius is assumed to be constant during the entire reaction.

2.3. The Valensi–Carter model

The only difference between the Valensi–Carter and Ginstling–Brounstein models is that, in the former, the assumption of a constant total particle radius is eliminated by introducing a ratio z. z is the volume of product formed per unit volume of reactant consumed, so that the instantaneous total radius of the sphere can be written as

$$r_{inst}=[zr_0^3+r^3(1-z)]^{1/3} \tag{12}$$

resulting in the differential equation

$$\frac{dr}{dt}=-k_3\left\{r-\frac{r^2}{[zr_0^3+r^3(1-z)]^{1/3}}\right\}^{-1} \tag{13}$$

where the rate constant is expressed as for the Ginstling–Brounstein (and Jander) model

$$k_3=\frac{D(c_2-c_1)}{\rho} \tag{14}$$

The integrated Valensi–Carter equation containing the degree of conversion instead of the core radius can be expressed as

$$[1+(z-1)x]^{2/3}+(z-1)(1-x)^{2/3}=z+\frac{2(1-z)k_3t}{r_0^2} \tag{15}$$

2.4. The phase-boundary reaction model

When the mass transport through the product layer is fast compared with the reaction rate, the kinetics can be modelled by a so-called phase-boundary model. The theory behind the phase-boundary model starts from an equation describing a first-order reaction. The consequence of this is that the interface between the product layer and the core moves with a constant radial velocity

$$\frac{dr}{dt}=-\frac{k_r c_1}{\rho} \tag{16}$$

where k_r is the first-order reaction constant, c_1 is the concentration of the reactant on the inner interface and ρ is the molar density of the reactant in the core. The integrated version of this model, including the degree of conversion, is given by the equation

$$k_4t=1-(1-x)^{1/3} \tag{17}$$

2.5. Combined mechanisms

It is probable that there is more than one mechanism controlling the reaction rate throughout the reaction process. One reasonable assumption is that, when the product layer is sufficiently thin, the diffusion of reactant through the product shell is faster than the reaction rate at the inner interface. This

means that, in the early stages of the reaction process, the kinetics can be described by the phase-boundary model since the product layer is thin at this point. As the reaction proceeds, the product layer becomes thicker and, at some point, the diffusive resistance becomes sufficiently large for the rate to become diffusion controlled. This mechanism has been suggested in the literature [5,17].

3. Experimental details

3.1. Sample preparation

Sodium carbonate was dissolved in distilled water. Titanium dioxide was added, the suspension was mixed using a magnetic stirrer and heated to the boiling point. Water started to evaporate and, after a while, the viscosity of the suspension increased greatly so that the magnetic stirrer could not be used. At this point, the sample was placed in a furnace (105 °C) to dry overnight. The sample was then ground to a fine powder. Two molar ratios were used: $TiO_2/Na_2CO_3 = 3$ for experiments carried out at temperatures below 800 °C, because the product at these temperatures is assumed to be $Na_2O \cdot 3TiO_2$, and $TiO_2/Na_2CO_3 = 1.25$ for experiments carried out at higher temperatures, because the main product in this case is assumed to be $4Na_2O \cdot 5TiO_2$ (or $Na_2O \cdot TiO_2$). The sample was analysed in order to determine the physical properties, e.g. particle size distribution (PSD) and particle size (see Section 4.1).

3.2. Equipment

The reaction was carried out in a tubular reactor made of quartz glass enclosed in a furnace; the technique was based on a concept used by Borgwart [18]. The quartz glass reactor consisted of three concentric pipes with the sample placed in a sample holder on the top of the innermost pipe (Fig. 2). The gas was heated as it flowed upwards between the two outer pipes before being forced down the inner pipe and through the sample, which rested on a porous bed of quartz glass inside the sample holder. A detailed description of the equipment and procedure can be found elsewhere [19].

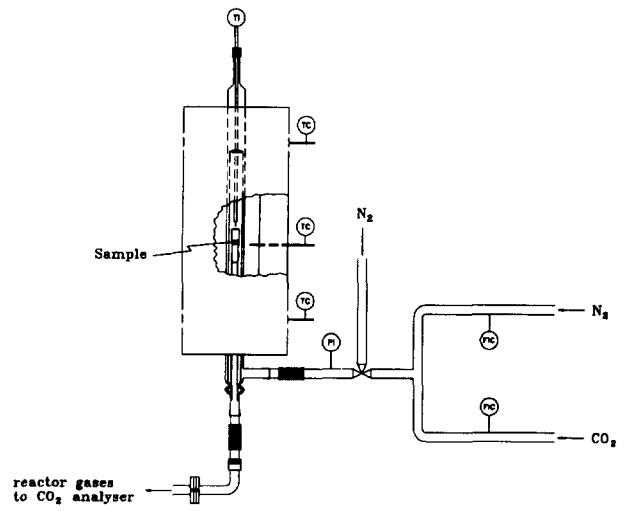

Fig. 2. The quartz glass reactor.

The mass flow of gas was determined by a mass flow controller (Brooks, models 5850E and 5851E) run by Brooks control and read out equipment.

The temperature inside the reactor was recorded by thermocouples and the accuracy of the measurements was about ±10 °C. The content of carbon dioxide in the reject gases from the reactor was measured using a non-dispersive infrared (NDIR) industrial photometer (URAS 3G, Mannesmann, Hartman and Braun). The signals from the measurements of the temperature, carbon dioxide concentration and mass flow were continuously registered every 4 s by a data acquisition unit.

3.3. Procedure

The nitrogen flow and furnace temperature were stabilized for more than 1 h at the beginning of each experimental session. A sample load of 0.70 g was placed in the sample holder. The amount of sample was chosen so as to obtain reproducible results from the measurements of the specific surface area of the sintered material. In order to obtain a porosity which was as similar as possible in all of the beds, the sample holder was gently shaken before being placed in the reactor.

The flow of nitrogen was interrupted when the conditions in the system were stable, and the sample holder was placed in the reactor as quickly as possible. The nitrogen flow was then increased to about 10 $l_{STP}\ min^{-1}$. It took approximately 50 s from the moment when the nitrogen was shut off until it reached the predetermined level.

When the reaction was completed, i.e. the carbon dioxide content in the reject gases was at the same level as before the sample was inserted, the gas flow was turned off and the sample holder was taken out of the reactor. The sample was cooled by flowing nitrogen and then weighed, still in the sample holder. The sample was then transferred immediately to a sample tube used for surface area measurements. The sample tube had been taken earlier from a drying oven, cooled and exposed to pure nitrogen gas for about 1 h. The sample was then degassed further in pure nitrogen before being weighed and analysed. The specific surface area of the product was measured by a five-point nitrogen adsorption method using a micromeretics Gemini 2370. Using the theory of Brunauer, Emmet and Teller, the surface area was calculated from measurements at five different pressures (BET surface area).

The investigated temperatures ranged from 690 to 880 °C. The experiments lasted from 30 min to 3 h. The concentration of carbon dioxide in the reject gases from the reactor varied from 0 to 6000 ppm. At least three tests were carried out for each combination of process conditions.

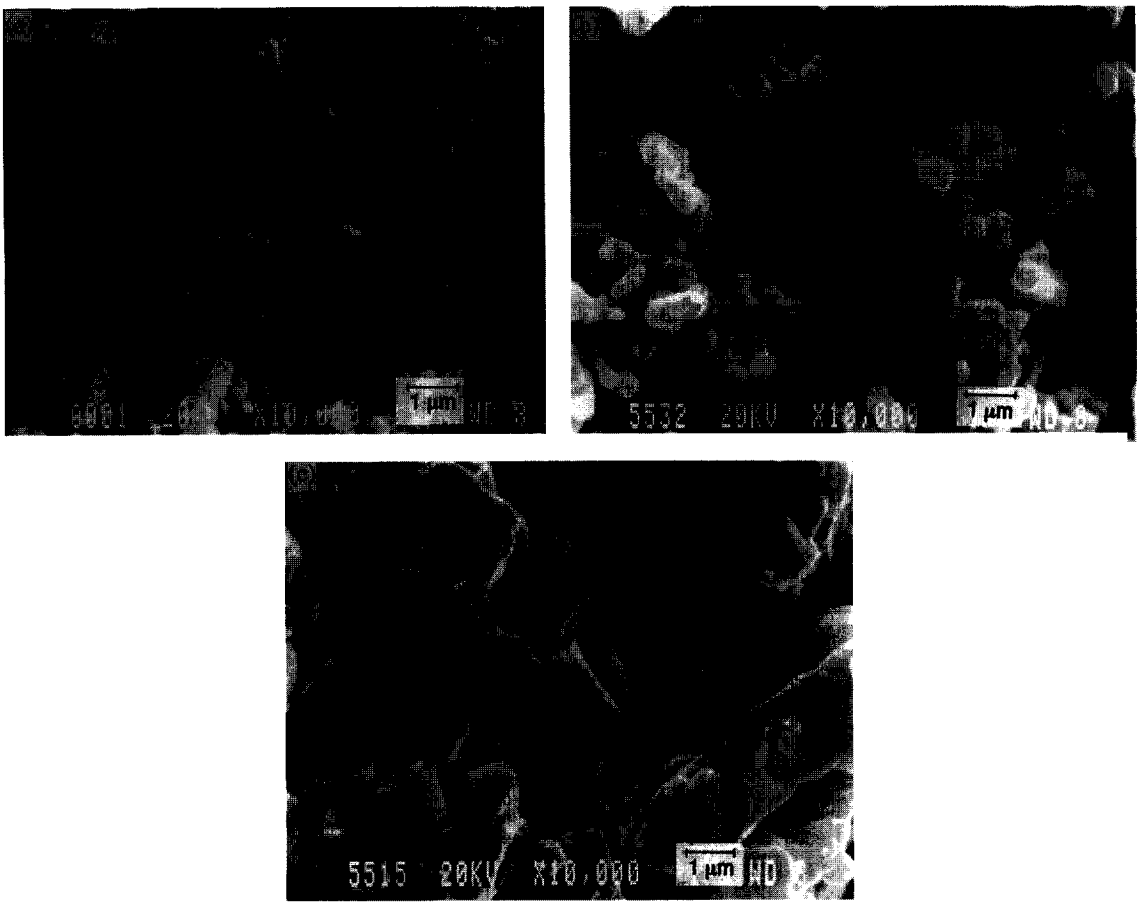

Fig. 3. (a) Scanning electron micrograph of unreacted, readily prepared material (magnification, 10 000×). (b) Scanning electron micrograph of product from the reaction at 800 °C (magnification, 10 000×). (c) Scanning electron micrograph of product from the reaction at 880 °C (magnification, 10 000×).

4. Results and discussion

4.1. Material characterization

A scanning electron micrograph of the readily prepared, unreacted material is shown in Fig. 3(a). Studies using scanning electron microscopy (SEM) indicate particles of relatively uniform size. By measuring the BET specific surface area and density of the material, and assuming the particles to be spherical, the average radius of the particles was estimated to be 0.32 μm. This is the radius used as the initial radius in the models. It was difficult to determine a PSD due to the small size of the particles. This, and the fact that the particle size did not vary greatly, meant that no consideration was given to the PSD in modelling the kinetics.

The scanning electron micrographs of the product shown in Fig. 3(b) and (c) illustrate the temperature dependence of the particle size during sintering. The material was not quite homogeneous, as particles sintered to form larger particles in some parts of the product sample.

The measurement of the BET specific surface area of the sintered product shows an increase with increasing temperature (Fig. 4). We assume that the difference in reaction mechanism at different temperatures can explain the slope variation at different temperatures.

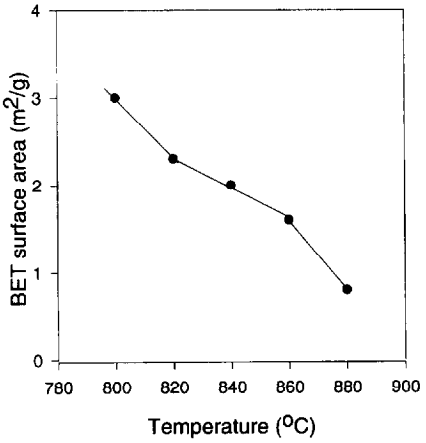

Fig. 4. Material sintering at different temperatures. The running time for these data was around 2000 s and the molar ratio was $TiO_2/Na_2CO_3 = 1.25$.

4.2. Product composition

The product composition was investigated by XRD. It should be pointed out that XRD results cannot be regarded as quantitative, but the dominating compounds can nevertheless be identified. The product from experiments carried out at 800 °C with a molar ratio $TiO_2/Na_2CO_3 = 1.25$ contained various titanates, e.g. $Na_2O \cdot 3TiO_2$ (PDF card 31-1329), $Na_2O \cdot TiO_2$ (PDF card 37-0345) and $Na_2O \cdot 6TiO_2$ (PDF

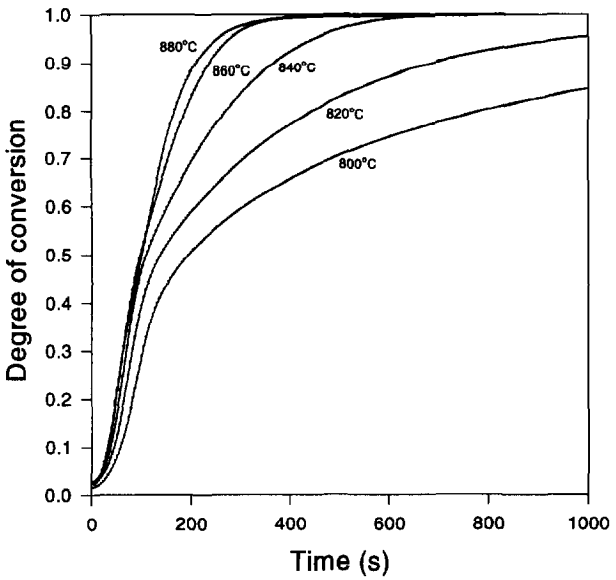

Fig. 5. Conversion of sodium carbonate vs. time in seconds for experiments carried out at 800, 820, 840, 860 and 880 °C. The molar ratio was $TiO_2/Na_2CO_3 = 1.25$.

card 37-0951). The product from runs at 840 °C showed an XRD pattern dominated by $4Na_2O \cdot 5TiO_2$, which is in accordance with earlier observations [5]. The product from runs carried out at 880 °C showed XRD patterns dominated by $Na_2O \cdot TiO_2$. At this temperature, when the reaction atmosphere is inert, this compound is the expected product. The results of XRD analysis confirm the occurrence of reactions (1), (2) and (6) in the temperature range studied.

4.3. Kinetic results

The kinetic results from experiments carried out at various temperatures between 800 and 880 °C are shown in Fig. 5. Preparations carried out at temperatures lower than 800 °C required more than 3 h to reach complete conversion as the reaction rate was relatively low at these temperatures. Complete conversion of sodium carbonate was obtained much more rapidly in the range 800–880 °C: in less than 1 h at 800 °C and in less than 10 min at 880 °C. The reaction could be carried out to complete conversion even when the reactants were in the solid state. Sodium carbonate melts at about 860 °C, titanium dioxide at 1840 °C and, for the titanates formed, the melting point is above 950 °C.

4.4. Modelling the kinetics

Earlier studies have shown that the Jander model based on diffusion-controlled kinetics gives the best fit for the reaction between titanium dioxide and sodium carbonate compared with models based on other rate-controlling mechanisms [5]. The Jander model, however, is based on diffusion in a plane sheet. The error for this model will be significant when the spherical product shell becomes thicker and the deviation from a plane sheet becomes significant. This error is eliminated with the Ginstling–Brounstein model, which is based on diffusion in a spherical shell. Furthermore, when titanium dioxide reacts with sodium carbonate to form the titanate phase, the volume increases by a factor of two, which can be found by measuring the densities of the reactant and product. The Ginstling–Brounstein model does not take this fact into account; it assumes that the particle radius is constant. This assumption is eliminated by the Valensi–Carter model. In this situation, the Valensi–Carter model is obviously the most complete of the three models discussed.

For this reason, the Valensi–Carter model was chosen as the best model in this study. The rate constant was determined by fitting the model to the experimental data by a computer program using the least-square method routine "leastsq" (Matlab). The reaction process was then simulated by a computer program written in FORTRAN that solved the Valensi–Carter differential equation numerically using the Runge–Kutta method. The relative errors for the model at the different temperatures were calculated as an average value between conversions from 9% to 96%; these are shown in Table 2. The best model fit was obtained at 840 °C (Fig. 6(a)) and the worst at 800 °C (Fig. 6(b)).

The rate constants obtained from model fitting were used to calculate the Arrhenius energy. An Arrhenius plot gives an almost straight line, except at the highest temperature of 880 °C (Fig. 7). The deviation at 880 °C is probably due to the fact that the reaction mechanism at this temperature is different, with meta-titanate formed as the main product according to reaction (6). A linear regression yields an Arrhenius energy of 206 kJ mol^{-1} if this value is omitted. This result can be compared with that of an earlier investigation of the same reaction for temperatures in the range 750–850 °C [5], where an Arrhenius energy of 208 kJ mol^{-1} was reported using the Jander model.

Table 2
Relative errors for the Valensi–Carter model and the combined model for experimental data obtained for five different temperatures

Temperature (°C)	Relative error (%) for the Valensi–Carter model	Relative error (%) for the combined model
800	8.1	5.1
820	4.8	3.7
840	2.1	0.9
860	5.0	1.8
880	7.9	4.8

The errors are average errors between degrees of conversion of 9% to 96%.

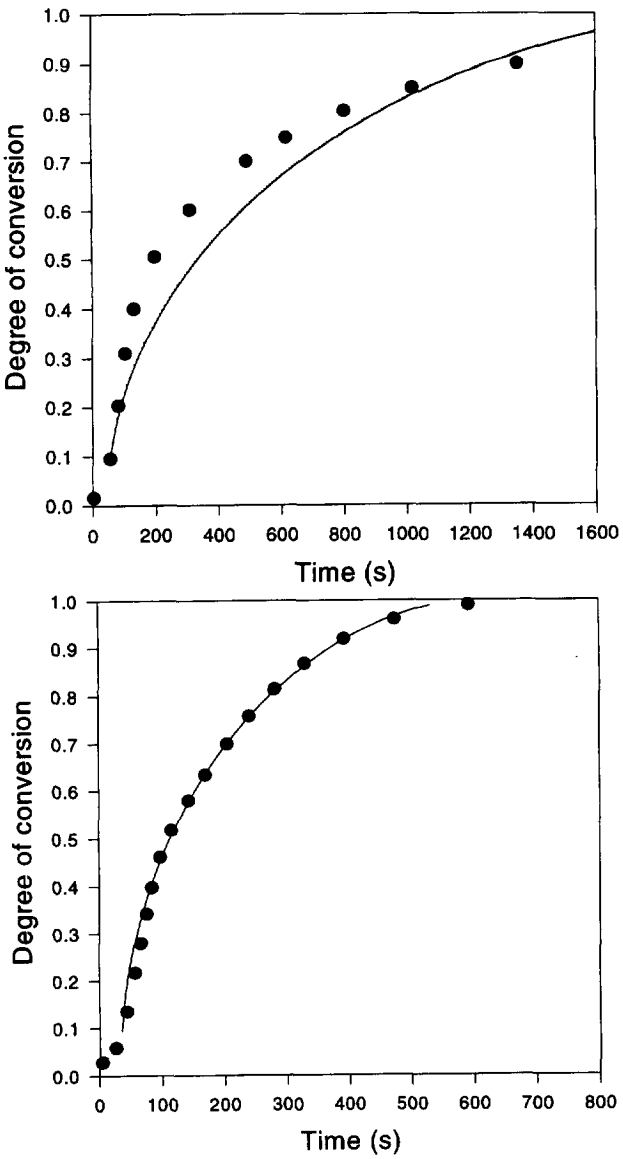

Fig. 6. (a) Valensi–Carter model (line) vs. experimental data (filled circles) at 800 °C. The molar ratio was $TiO_2/Na_2CO_3 = 1.25$. (b) Valensi–Carter model (line) vs. experimental data (filled circles) at 840 °C. The molar ratio was $TiO_2/Na_2CO_3 = 1.25$.

If the initial stage of the reaction process is not controlled by diffusion, as a result of the fast diffusion in the thin product layer, this early stage could be described by the phase-boundary model; at a certain point, the diffusion-controlled mechanism starts to dominate. Such a model was developed and a FORTRAN simulation program was constructed. In this program, the mechanism changes abruptly when the product shell becomes sufficiently thick. The early stage of the reaction was described using phase-boundary kinetics and the second part of the reaction was modelled using Valensi–Carter kinetics. The result revealed a better fit than the model with only one mechanism considered. The relative errors are shown in Table 2; these errors are average values between degrees of conversion in the range 9%–96%. The relative error at 840 °C is less than 1%. A comparison between the

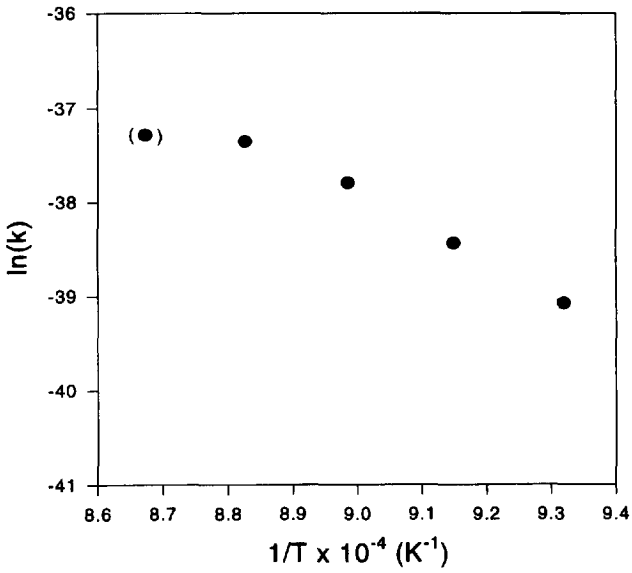

Fig. 7. Arrhenius plot based on the rate constants for the Valensi–Carter model.

calculated and measured data at this temperature is shown in Fig. 8.

As shown in Table 2, both models work well for temperatures of around 840 °C, with errors increasing for the highest (880 °C) and lowest (800 °C) temperatures. The reaction mechanism is not the same at different temperatures in the 800–880 °C range: at 840 °C, the main reaction product is penta-titanate ($4Na_2O \cdot 5TiO_2$); at 880 °C, the main reaction product is meta-titanate ($Na_2O \cdot TiO_2$). This indicates that the kinetic mechanism is different for different temperatures in accordance with the diversity in model fitting.

5. Conclusions

It has been shown experimentally that the direct causticization reaction between sodium carbonate and titanium dioxide can be accomplished to complete conversion below the melting point of sodium carbonate. However, the reaction is faster for temperatures around and above the melting point of sodium carbonate (complete within 10 min). A theoretical comparison of three models based on diffusion-controlled kinetics was presented and the Valensi–Carter model was suggested to be the best and most complete model. The Valensi–Carter model was used to describe the reaction between sodium carbonate and titanium dioxide, and gave a good fit to the experimental data. An Arrhenius plot analysis was carried out using this model, and the Arrhenius energy was estimated to be 206 kJ mol^{-1}. Finally, a model based on phase-boundary kinetics in the initial stage of the reaction and diffusion-controlled kinetics according to Valensi–Carter in the final stage of the reaction process was presented. This model had an average relative error of less than 1% for conversions between 0.09 and 0.96 for experimental data at 840 °C. Above and below 840 °C, the errors increased for both

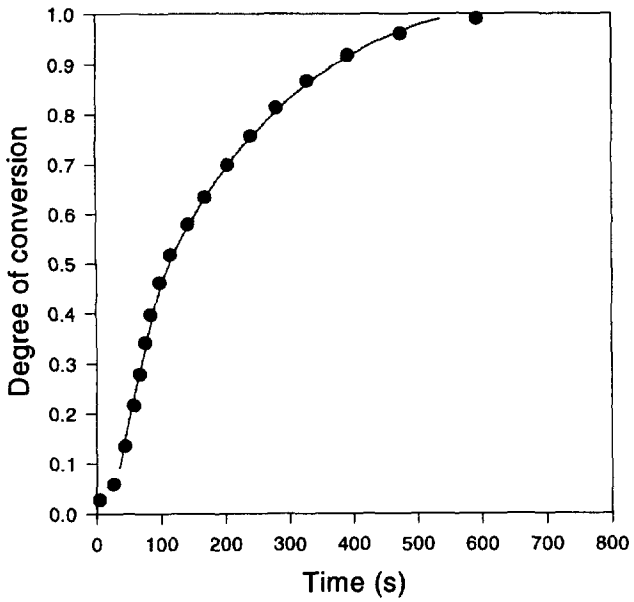

Fig. 8. A combined phase-boundary and Valensi–Carter model (line) vs. experimental data at 840 °C (filled circles). The molar ratio was $TiO_2/Na_2CO_3 = 1.25$.

the Valensi–Carter and combined models. We assume that the reasons for this are the different reaction mechanisms at different temperatures.

Acknowledgements

The authors thank the Swedish Black Liquor Research Programme for financial support.

Appendix A. Nomenclature

c	concentration (mol m^{-3})
D	diffusivity (m^2 s^{-1})
r	core radius, spherical coordinate (m)
r_0	initial radius of the sphere (m)
t	time (s)
z	volume of product formed per volume reactant consumed
ρ	molar density (mol m^{-3})

References

[1] G.H. Covey, Development of the direct alkali recovery system and potential applications, Pulp Paper Canada 83 (12) (1982) T350.
[2] K.N. Maddern, Mill-scale development of the DARS direct causticization process, Pulp Paper Canada 87 (10) (1986) 78.
[3] R.E. Scott-Young, M. Cukier, Commercial development of the DARS process, Int. Chem. Recov. Conf., 1995, p. B263.
[4] E. Kiiskilä, Recovery of sodium hydroxide from alkaline pulping liquors by smelt causticizing, part II. Reactions between sodium carbonate and titanium dioxide, Paperi ja Puu - Papper och Trä 61 (5) (1979) 394.
[5] X. Zou, Recovery of kraft black liquor including direct causticization, Ph.D. Thesis, Department of Chemical Engineering, McGill University, Montreal, Quebec, Canada, 1991.
[6] C.E. Bamberger, G.M. Begun, Sodium titanates: stoichiometry and Raman spectra, J. Am. Ceram. Soc. 70 (3) (1987) C-48.
[7] E.K. Belayev, The formation of sodium metatitanate in sodium carbonate–titanium dioxide mixings, Russ. J. Inorg. Chem. 21 (1976) 830.
[8] A. Amin, M.A. Spears, B.M. Kulwicki, Reaction of anatase and rutile with barium carbonate, J. Am. Ceram. Soc. 66 (10) (1983) 733.
[9] G.W. Brindley, R. Hayami, Kinetics and mechanism of formation of forterite (Mg_2SiO_4) by solid state reaction of MgO and SiO_2, Philos. Mag. 12 (1965) 505.
[10] E.A. Cooper, T.O. Mason, Mechanism of La_2CuO_4 solid-state powder reaction by quantitative XRD and impedance spectroscopy, J. Am. Ceram. Soc. 78 (4) (1995) 857.
[11] B. Freudenberg, A. Mocellin, Aluminium titanate formation by solid-state reaction of fine Al_2O_3 and TiO_2 powder, J. Am. Ceram. Soc. 70 (1) (1987) 33.
[12] W. Jander, Reactions in solid state at high temperatures: I, Z. Anorg. Allg. Chem. 163 (1927) 1 (in German).
[13] E.R. McCartney, L.K. Templeton, J.A. Pask, The solid-state reaction between barium metatitanate and barium carbonate to form barium orthotitanate, Proceedings Fourth International Symposium Reactivity of Solids, Amsterdam, 1960, Elsevier, 1961, p. 672.
[14] H. Tagawa, K. Igarashi, Reaction of strontium carbonate with anatase and rutile, J. Am. Ceram. Soc. 69 (4) (1986) 310.
[15] S.S. Tamhankar, L.K. Doraiswamy, Analysis of solid–solid reactions: a review, AIChE J. 25 (1979) 561.
[16] R.E. Carter, Kinetic model for solid-state reactions, J. Chem. Phys. 34 (1961) 2010.
[17] D.L. Fresh, J.S. Dooling, Kinetics of the solid-state reaction between magnesium oxide and ferric oxide, J. Phys. Chem. 70 (1966) 3198.
[18] R.H. Borgwart, Calcium oxide sintering in atmospheres containing water and carbon dioxide, Ind. Eng. Chem. Res. 28 (1989) 493.
[19] C. Hansson, Lime mud reburning—properties and quality of the lime produced, Ph.D. Thesis, Department of Chemical Engineering Design, Chalmers University of Technology, Göteborg, Sweden, 1993.